Pyrazole Formation: Examination of Kinetics, Substituent Effects, and Mechanistic Pathways

JOSEPH C. SLOOP,[1] BRENT LECHNER,[1] GARY WASHINGTON,[1] CARL L. BUMGARDNER,[2] W. DAVID LOEHLE,[1] WILLIAM CREASY[3]

[1]*Department of Chemistry, United States Military Academy, West Point*, NY 10996
[2]*Department of Chemistry, North Carolina State University, Raleigh*, NC 27695
[3]SAIC, P.O. *Box* 68, *Gunpowder Branch, Aberdeen Proving Ground*, MD 21010

Received 2 October 2007; revised 14 November 2007, 7 January 2008; accepted 10 January 2008

DOI 10.1002/kin.20316
Published online in Wiley InterScience (www.interscience.wiley.com).

ABSTRACT: Reaction kinetics for the condensation of 1,3-diketones **1a–o** with selected arylhydrazines (aryl = Ph, 4-NO_2Ph, 4-CH_3OPh, and 2,4-diNO_2Ph) was studied using ^{19}F NMR spectroscopy. Product regioselectivity is modulated by reactant ratios, substituents, and acidity. Reaction rates were found to be influenced by substituents on the diketones and on phenylhydrazines as well as by acidity of the reaction medium with rates varying as much as 1000-fold. Hammett ρ values for these cyclizations were determined. The reaction was found to be first order in both the diketone and arylhydrazine. The rate-determining step for pyrazole formation shifts as a function of pH. Mechanistic details and reaction pathways supporting these findings are proposed. © 2008 Wiley Periodicals, Inc. Int J Chem Kinet 40: 370–383, 2008

INTRODUCTION

N-Phenylpyrazoles, which are important precursors to pharmaceuticals and pesticides [1–5],[1] can be easily prepared by the condensation of dicarbonyl species with hydrazine derivatives. Although pyrazole synthesis has been studied extensively [6–13], kinetics investigations of this condensation beyond phenylhydrazone (**II**) formation have been qualitative in nature [10–16].

While preparing pyrazoles under acidic conditions [3,6,7,13] from selected diketones [17] (Scheme 1), we noted variations in product formation rates and regioselectivity, prompting us to undertake a comprehensive kinetics study of this reaction (Scheme 2). Our principal efforts were directed at quantifying influences that substituted diketones, substituted phenylhydrazines, and pH exert on the reaction rate. Finally, we propose mechanistic pathways for this condensation that are consistent with experimental observations.

The views expressed in this academic research paper are those of the authors and do not necessarily reflect the official policy or position of the U.S. Government, the Department of Defense, or any of its agencies.

Correspondence to: Joseph C. Sloop; e-mail: joseph.sloop@usma.edu.

Contract grant sponsor: U.S. Military Academy Faculty Research Fund.

[1]Preliminary studies show cytotoxicity toward plant and animal cell lines below [pyrazole] = 10^{-6} M.

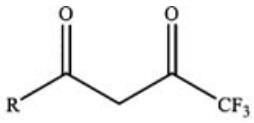

1a: R = CH_3, **1b**: R = C_2H_5, **1c**: R = i-C_3H_7, **1d**: R = i-C_4H_9, **1e**: R = n-C_6H_{13}, **1f**: R = t-C_4H_9, **1g**: R = Ph, **1h**: R = 2-FPh, **1i**: R = 2-CH_3Ph, **1j**: R = 2-CH_3OPh, **1k**: R = 4-FPh, **1l**: R = 4-CH_3Ph, **1m**: R = 4-CH_3OPh, **1n**: R = 4-CNPh, **1o**: R = 4-NO_2Ph

Scheme 1 Trifluoromethyl-1,3-diketones.

EXPERIMENTAL

NMR data were collected using a Varian VXR-200 spectrometer using $CDCl_3$ as an internal standard unless otherwise noted (^{19}F: 168 MHz in ethanol w/$CFCl_3$ as an external standard, ^{13}C: 50.2 MHz, ^{1}H: 200 MHz) and/or Brüker Avance 300 spectrometer (^{19}F: 252 MHz in CF_3CH_2OH as an internal standard, ^{13}C: 75.4 MHz, ^{1}H: 300 MHz). UV–visible spectrophotometric data were collected by a Hewlett-Packard 8452A diode array and/or an Agilent 8453 spectrophotometer. Solution pH was determined using an Orion SA520 pH meter with a polymer body sealed combination reference electrode and were calibrated using standard buffer solutions at pH 3–6. Melting points were obtained from a Mel-temp apparatus and are uncorrected.

General Procedures for the Preparation of Pyrazoles (Unbuffered, pH 1.6)

To a 10-mL volumetric flask equipped with a magnetic stirrer, 8–9 mL 95% ethanol was added, followed by addition of approximately 2.0 mmol of the 1,3-diketone (**1a–o**) [7,17] and 0.01 mL of concentrated H_2SO_4. Then, an equimolar amount of the hydrazine was added and the solution was diluted to 10 mL while stirring at 25°C. NMR data were collected at 180-s intervals. Reaction mixtures were neutralized with saturated $NaHCO_3$, extracted with CH_2Cl_2, dried over $MgSO_4$, the solvent was removed under reduced pressure, and then distilled or recrystallized from EtOH.

3-Methyl-1-phenyl-5-trifluoromethylpyrazole (**2a**) and 5-methyl-1-phenyl-3-trifluoromethylpyrazole (**3a**) [11]: These compounds were obtained as a brownish liquid (1:1 mixture of **2a:3a**), bp 133–135°C (28 mmHg) (lit. [7], bp 133°C (28 mmHg)).

3-Ethyl-1-phenyl-5-trifluoromethylpyrazole (**2b**) and 5-ethyl-1-phenyl-3-trifluoromethylpyrazole (**3b**): These compounds were obtained as a yellow liquid (38:62 mixture of **2b:3b**). Distillation yields a 62:38 mixture of **2b:3b**, bp 175–177°C (25 mmHg) (lit. [7], bp 175–177°C (25 mmHg)).

3-Isopropyl-1-phenyl-5-trifluoromethylpyrazole (**2c**) and 5-isopropyl-1-phenyl-3-trifluoromethylpyrazole (**3c**): These compounds were obtained as a pale yellow liquid, which on distillation yielded a 88:12 mixture of **2c:3c**, bp 198–200°C (lit. [7], bp 198°C).

3-Isobutyl-1-phenyl-5-trifluoromethylpyrazole (**2d**) and 5-isobutyl-1-phenyl-3-trifluoromethylpyrazole (**3d**): These compounds were obtained as a yellow liquid (30:70 mixture of **2d:3d**), bp 161–164°C (25 mmHg) (lit. [7], bp 161–164°C (25 mmHg)).

3-Hexyl-1-phenyl-5-trifluoromethylpyrazole (**2e**) and 5-hexyl-1-phenyl-3-trifluoromethylpyrazole (**3e**): These compounds were obtained as a pale yellow liquid (27:72 mixture of **2e:3e**), bp 180–183°C (lit. [7], bp 181–184°C).

5-t-Butyl-1-phenyl-3-trifluoromethylpyrazole (**3f**): This compound was obtained as white crystals (EtOH), **3f**, mp 121–123°C (lit. [7], mp 121–123°C).

1,3-Diphenyl-5-trifluoromethylpyrazole (**2g**) and 1,5-diphenyl-3-trifluoromethyl-pyrazole (**3g**): These compounds were obtained as an 18:82 mixture of **2g:3g**, which on recrystallization (EtOH) gave white crystals, **3g**, mp 87–88°C (lit. [3], mp 95°C).

5-(2-Fluorophenyl)-1-phenyl-3-trifluoromethylpyrazole (**3h**): This compound was obtained as a pale purple solid; **3h**, mp 80–83°C (lit. [7], mp 80–83°C).

5-(2-Methylphenyl)-1-phenyl-3-trifluoromethylpyrazole (**3i**): This compound was obtained as

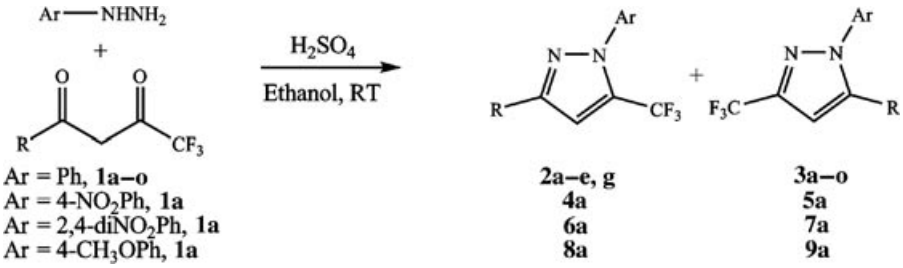

Ar = Ph, **1a–o**
Ar = 4-NO_2Ph, **1a**
Ar = 2,4-diNO_2Ph, **1a**
Ar = 4-CH_3OPh, **1a**

2a–e, g
4a
6a
8a

3a–o
5a
7a
9a

Scheme 2 Condensation of trifluoromethyl-1,3-diketones with arylhydrazines.

yellow crystals (EtOH); **3i**, mp 56–58°C (lit. [7], mp 56–58°C).

5-(2-Methoxyphenyl)-1-phenyl-3-trifluoromethylpyrazole (**3j**): This compound was obtained as a pale yellow liquid; **3j**, bp 159°C (28 mmHg) (lit. [7], bp 159°C (28 mmHg)).

5-(4-Fluorophenyl)-1-phenyl-3-trifluoromethylpyrazole (**3k**): This compound was obtained as a yellow solid; **3k**, mp 101°C (lit. [7], mp 101°C).

5-(4-Methylphenyl)-1-phenyl-3-trifluoromethylpyrazole (**3l**): This compound was obtained as a yellow liquid; **3l**, bp 165°C (28 mmHg) (lit. [7], bp 165°C (28 mmHg)).

5-(4-Methoxyphenyl)-1-phenyl-3-trifluoromethylpyrazole (**3m**): This compound was obtained as a pale yellow liquid; **3m**, bp 159°C (28 mmHg) (lit. [7], bp 159°C (28 mmHg)).

5-(4-Cyanophenyl)-1-phenyl-3-trifluoromethylpyrazole (**3n**): This compound was obtained as a yellow solid (EtOH); **3n**, mp 77°C (lit. [7], mp 77°C).

5-(4-Nitrophenyl)-1-phenyl-3-trifluoromethylpyrazole (**3o**): This compound was obtained as a yellowish-brown solid; **3o**, mp 56°C (lit. [7], mp 56°C).

3-Methyl-1-(4-nitrophenyl)-5-trifluoromethylpyrazole (**4a**) and 5-methyl-1-(4-nitrophenyl)-3-trifluoromethylpyrazole (**5a**) [11]: These compounds were obtained as a yellowish-brown solid (1:1 mixture of **4a:5a**), mp 52–54°C (lit. [7], mp 52–54°C).

1-(4-Methoxyphenyl)-3-methyl-5-trifluoromethylpyrazole (**6a**) and 1-(4-methoxyphenyl)-5-methyl-3-trifluoromethylpyrazole (**7a**): These compounds were obtained as a 1:1 mixture of **6a:7a**, which, upon recrystallization (EtOH), yielded white crystals; **7a**, mp 66–69°C (lit. [7], mp 66–69°C).

3-Methyl-1-(2,4-dinitrophenyl)-5-trifluoromethylpyrazole (**8a**) and 5-methyl-1-(2,4-dinitrophenyl)-3-trifluoromethylpyrazole (**9a**): These compounds were obtained as a 4:1 mixture of **8a:9a**, which, upon recrystallization (EtOH), yielded yellow crystals; **8a**, mp 94–97°C (lit. [7], mp 95–98°C).

Initial Rates Method for Pyrazole Kinetics Study (Unbuffered, pH 1.6)

Reaction solutions were prepared [7,17] and their progress measured by NMR as described above. The NMR data were collected at 180-s intervals. Because the starting diketones, all intermediates and products contained fluorine (as the $-CF_3$ moiety) in the same molar ratios, the concentrations of each species could be monitored simultaneously throughout the reaction by ^{19}F NMR. Direct integrations of the ^{19}F signal for each component afforded intensities (I), which were related to the concentrations by the following equation: $C_i = (I_i/I_T)C_0$, where $I_T = \Sigma I_i$ and C_0 is the initial diketone concentration. In the cases of **1h** and **1k**, the ^{19}F signal due to the aromatic fluorine was outside the range of chemical shifts considered and, therefore, not part of the total fluorine integrations. These concentrations were plotted versus time, and the initial rate obtained as the slope of a best-fit line to the earliest linear portion of the data ($t < 600$ s).

Isolation Method for Pyrazole Reaction Order Determination (Unbuffered, pH 1.6)

Reaction solutions of **1a** and phenylhydrazine were prepared [7,17], and their progress was measured by NMR as described above. To determine the reaction order with respect to the diketone, the concentration of the diketone was doubled to 400 mM while the other reactant concentrations were held constant: $[PhNH_2NH_2] = 200$ mM, $[H^+] = 25$ mM. To determine the reaction order with respect to phenylhydrazine, the concentration of phenylhydrazine was doubled to 400 mM while the other reactant concentrations were held constant: [**1a**] = 200 mM, $[H^+] = 25$ mM. Initial rates for these runs were determined as above and compared.

Buffer Studies

To a 10-mL volumetric flask equipped with a magnetic stirrer, 8–9 mL 95% ethanol/buffer solution (pH 1, 2, 3, 3.3, 4, 5, and 6) was added, followed by addition of approximately 2.0 mmol of the diketone **1a**. Then, an equimolar amount of phenylhydrazine was added and the solution was diluted to 10 mL while stirring at 25°C. NMR data were collected at 180-s intervals. Measured pH values were accurate to within ±0.05 pH unit.

General Procedures for the Isolation of Reaction Intermediates

Reaction conditions used were those given in the section above except as noted below. The arylhydrazine (1 eq.) was added to **1a** in ethanol at pH ~6, and the reaction was allowed to proceed for ~1 min. The temperature of the reaction vessel was lowered to 0°C, precipitating the arylhydrazone products from solution. The products were filtered, dried under a stream of nitrogen, subjected to radial chromatography as required, and characterized. All intermediates were resubjected to reaction conditions ca. pH 2 and found to give the corresponding known pyrazole products.

4-Phenylhydrazono-1,1,1-trifluoro-2-pentanone (**II-2-2a**). This compound was obtained as a yellow oily solid, mp 35–39°C. **II-2-2a**: NMR: δ ^{1}H: 0.94 (3H, s), 2.42 (2H, s), 7.32 (5H, m), 10.8 (1H, bs). ^{13}C: δ 16.1, 117.7 (q, $^1J_{C-F} = 269$ Hz), 118.2, 119.1, 130.3, 142.4, 153.4, 206.7 (q, $^2J_{C-F} = 33$ Hz).^{19}F (CF_3CH_2OH): δ −80.3 (3F, s), UV: λ_{max}(EtOH) = 322 nm. HRMS (EI^+): calcd for $C_{11}H_{11}F_3N_2O$: 244.0823, found 244.0820.

4-(4-Nitrophenylhydrazono)-1,1,1-trifluoro-2-pentanone (**II-2-4a**). This compound was obtained as an orange-brown solid, mp 110–115°C dec. **II-2–a**: NMR: δ ^{1}H: 1.1 (3H, s), 2.5 (2H, s), 7.39 (2H, d, $J = 8.8$ Hz), 7.97 (2H, d, $J = 8.8$ Hz), 10.5 (1H, bs). ^{13}C: δ 16.6, 20.3, 116.9 (CF_3, q, $^1J_{C-F} = 261$ Hz), 117.3, 124.8, 137.6, 149.8, 153.2, 206.2 (q, $^2J_{C-F} = 34$ Hz).^{19}F: δ −80.4 (3F, s), UV: λ_{max}(EtOH) = 328 nm. HRMS ($EI^{+)}$: calcd for $C_{11}H_{10}F_3N_3O_3$: 289.0674, found 290.0675.

4-(2,4-Dinitrophenylhydrazono)-1,1,1-trifluoro-2-pentanone (**II-2-6a**). This compound was obtained as an orange solid, mp 210–217°C dec. **II-2-6a**: NMR: δ ^{1}H: 1.25 (3H, s), 2.39 (2H, s), 7.79 (1H, d, $J = 9.0$ Hz), 8.31 (1H, d, $J = 9.0$ Hz), 8.98 (1H, s), 11.46 (1H, bs). ^{13}C: δ 17.1, 33.2, 117.4 (CF_3, q, $^1J_{C-F} = 271$ Hz), 118.2, 121.1, 131.0, 137.9, 139.4, 145.9, 154.2, 205.1 (q, $^2J_{C-F} = 35$ Hz). ^{19}F: δ −80.5 (3F, s), UV: λ_{max}(EtOH) = 371 nm. HRMS (EI^+): calcd for $C_{11}H_9F_3N_4O_5$: 334.0525, found 334.0526.

5-Methyl-2-(4-nitrophenyl)-3-trifluoromethyl-3,4-dihydro-2*H*-pyrazol-3-ol (**III-2-4a**): The ethanolic solution was extracted with diethyl ether, dried over Na_2SO_4 and the solvent was removed under reduced pressure. Recrystallization (diethyl ether) yielded brown crystals. **III-2–4a**: mp 103°C, (lit. [11], mp 102°C). NMR: δ ^{1}H: 1.75 (1H, bs), 2.11 (3H, s), 3.18 (1H, d, $^1J = 18.9$ Hz), 3.53 (1H, d, $^1J = 18.9$ Hz), 7.46 (2H, d, $^2J = 9.4$ Hz), 8.05 (2H, d, $^2J = 9.4$ Hz). ^{13}C: δ 14.8, 17.0, 85.8, 114.8, 122.9 (CF_3, q, $^1J_{C-F} = 269$ Hz), 123.8, 144.8 (CF_3, q, $^2J_{C-F} = 39$ Hz), 150.5, 208.7.^{19}F: δ −81.6 (3F, s).

RESULTS AND DISCUSSION

Pyrazole Formation Kinetic Studies

Reaction progress for the condensation in Scheme 2 was conveniently monitored by ^{19}F NMR. See the example spectra in Fig. 1 depicting the starting diketone equilibrium mixture of **1a** in acidic ethanol (Fig. 1a) and the reaction mixture of **1a** with phenylhydrazine at various times (Figs. 1b–1d). Product formation was followed by development of ^{19}F NMR signals (referenced to $CFCl_3$) near −57 and −62 ppm [7,9],[1] which correspond to the two possible pyrazole regioisomers, compound series **2** and **3**, respectively. In addition, several intermediates were observed by ^{19}F NMR during this cyclization (see Fig. 1b). Key among them were arylhydrazones [10,18] **II-2** and **II-3**, which were identified by NMR[2] and their rate of disappearance compared with that of product formation [6,7,9]. Small amounts of the transient carbinolamine intermediates (**I**) and pyrazoline intermediates (**III**) were also identified [10].

Of particular note here in Fig. 1b is the rapid loss of **1a**, the small quantities of carbinolamine intermediates (**I**), and the rapid formation of the phenylhydrazone intermediates (**II**). Previous work has shown that rate constants for phenylhydrazone formation are ca. 10^3 M^{-2} s^{-1} [19]. We will see presently how this compares with our measured product formation rate constants. By $t = 2$ h (Fig. 1c), carbinolamines **I-2** and **I-3** are depleted and **II-2** and **II-3** are the major nonproduct species in the reaction medium. The pyrazoline intermediates (**III**), while present at $t = 2$ h, are not found in the final reaction mixture (Fig. 1d). We will discuss the implications of these facts later.

Effect of Diketone Substituents on the Reaction Rate and Product Distribution

From the NMR data, pyrazole formation rates for a number of trifluoromethyl-1,3-diketones with phenylhydrazines in acidic ethanol were determined. The consumption rates of intermediates **II-2** and **II-3**, rates of product formation, observed rate constant, k_{obs}, and relative rates are presented in Table I.

The reaction order with respect to both the diketone and phenylhydrazine was determined using the isolation and initial rates methods. The data are collected in Table II. The reaction was found to be first order in both diketone and phenylhydrazine, where

$$\text{Rate} = k_{obs}[\text{diketone}][\text{phenylhydrazine}]$$

and k_{obs} is a second-order rate constant.

Examination of the data in Table I (entries 1–15) and Table II allows us to make several different comparisons. First, pyrazole **3** is formed faster than pyrazole **2**.

[1] Chemical shift differences of approximately 2 ppm were noted under the acidic, ethanolic reaction conditions relative to $CDCl_3$. See [19] for additional information.

[2] The hydrazone intermediates were isolated by lowering the temperature of the reaction vessel to 0°C. Solid hydrazone products (**II-2, II-4, II-6**) precipitated from solution were filtered, dried, and identified by ^{19}F, ^{1}H, and ^{13}C NMR.

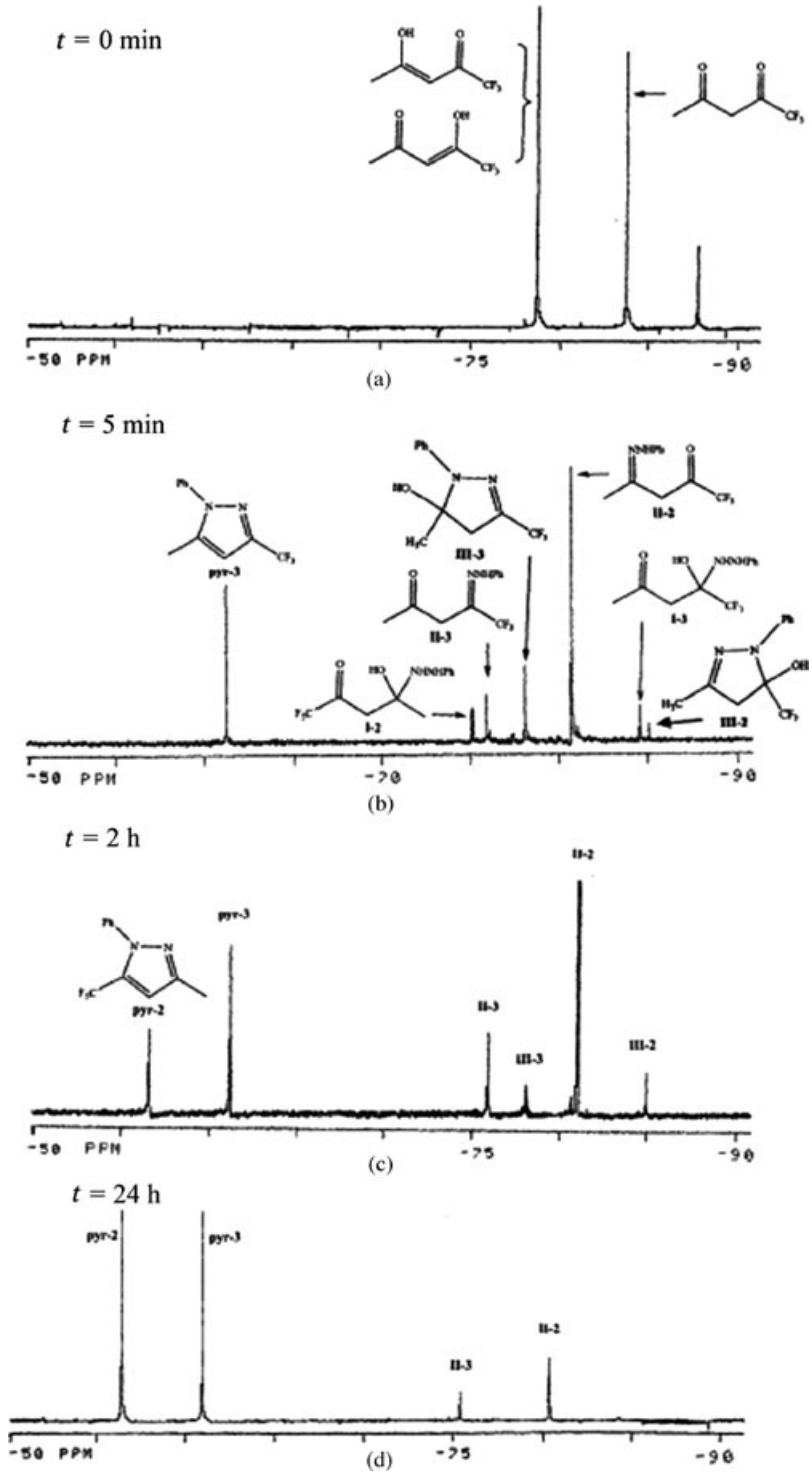

Figure 1 ^{19}F NMR spectra of **1a** and phenylhydrazine in ethanol.

This is consistent with preferential initial nucleophilic attack by the phenylhydrazine at the more electrophilic carbonyl, adjacent to the trifluoromethyl group.

In general, we found that aliphatic trifluoromethyl-1,3-diketones react more rapidly than the aromatic diketones. Apparently, the extrastability accrued through conjugation of the aromatic ring with the carbonyl lowers the reactant ground state energy so that the reaction proceeds more slowly in aromatic cases. To verify this, we carried out B3LYP/6-31G*

Table I Pyrazole Formation Kinetic Data[a]

Entry	Pyrazole (%)[b]	R^c	$-d\mathbf{II}_2/dt$ (mM s^{-1})	dP_2/dt (mM s^{-1})	$-d\mathbf{II}_3/dt$ (mM s^{-1})	dP_3/dt (mM s^{-1})	dP_T/dt (mM s^{-1})	$k_{obs}{}^d$ (mM s^{-1})$^{c-}$	$k/k_0{}^e$
1	**2a**(50%)/**3a**(50%)	CH_3	0.001	0.001	0.14	0.14	0.141	3.5	32
2	**2b**(38%)/**3b**(62%)	C_2H_5	0.014	0.013	0.085	0.086	0.099	2.3	29
3	**2c**(12%)/**3c**(88%)	$CH(CH_3)_2$	0.002	0.002	0.037	0.036	0.038	0.95	8.6
4	**2d**(30%)/**3d**(70%)	$CH_2CH(CH_3)_2$	0.002	0.002	0.037	0.038	0.040	1.0	9.9
5	**2e**(27%)/**3e**(72%)	n-C_6H_{13}	–	0.001	–	0.063	0.064	1.6	14
6	**3f**	$C(CH_3)_3$	–	–	0.026	0.026	0.026	0.65	5.9
7	**2g**(18%)/**3g**(82%)	Ph	0.0003	0.0003	0.0042	0.0041	0.0044	0.11	1.0
8	**3h**	2-FPh	–	–	0.0040	0.0041	0.0041	0.10	0.91
9	**3i**	2-CH_3Ph	–	–	0.0024	0.0024	0.0024	0.060	0.55
10	**3j**	2-CH_3OPh	–	–	0.0023	0.0022	0.0022	0.055	0.50
11	**3k**	4-FPh	–	–	0.0030	0.0029	0.0029	0.073	0.66
12	**3l**	4-H_3CPh	–	–	0.0028	0.0018	0.0018	0.045	0.41
13	**3m**	4-H_3COPh	–	–	0.0013	0.0013	0.0013	0.033	0.30
14	**3n**	4-NCPh	–	–	0.037	0.037	0.037	0.93	8.5
15	**3o**	4-O_2NPh	–	–	0.067	0.068	0.068	1.7	15
16	**4a**(50%)/**5a**(50%)	CH_3	0.0009	0.0009	0.0039	0.004	0.0049	0.12	0.035[f]
17	**6a**(80%)/**7a**(20%)	CH_3	0.0008	0.0008	0.0028	0.0028	0.0036	0.089	0.024[f]
18	**8a**(50%)/**9a**(50%)	CH_3	0.19	0.20	1.21	1.21	1.41	35.3	10.2[f]

[a] [Reactant] = 0.20 M, [acid] = 0.025 M, 298 K.
[b] Product distributions are those obtained prior to distillation or other purification.
[c] See Scheme 1.
[d] k_{obs} determined from total product formation rate, $dP_2/dt + dP_3/dt = dP_T/dt$.
[e] Rates relative to entry 7.
[f] Rates relative to entry 1.

Table II Determination of Pyrazole Formation Reaction Order[a]

$[C]_0$ (mM)		ν_0 (mM s^{-1})				
$[PhNH_2NH_2]_0$	$[CH_3COCH_2COCF_3]_0$	$-dII_2/dt$	dP_2/dt	dII_3/dt	dP_3/dt	dP_T/dt
200	200	0.0010	0.0010	0.140	0.140	0.141
200	400	0.0021	0.0020	0.279	0.281	0.283
400	200	0.0020	0.0019	0.278	0.279	0.280

[a] $[H^+]$ = 25 mM for all runs.

computations[3] on compounds **1a** and **1g** in ethanol. The total standard Gibbs free energies shown in Table III indicate that compound **1g** is lower in energy than **1a**. The equilibrium constants (K_{eq}) show that both diketo and enolic forms are likely to be present in the reaction medium. Cartesian coordinates, vibrational analyses, and other computational parameters for the diketo and enol tautomers of **1a** and **1g** are provided in the supplemental material.[4]

Table III Total Standard Gibbs Free Energies (kcal/mol) for Diketone Tautomers of **1a** and **1g** in Ethanol

Compounds	R	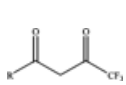 G_{Total}	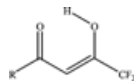 K_{eq}	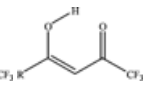 K_{eq}
1a	CH_3	−403512.6050	0.56347	4.49052
1g	Ph	−523964.4896	0.97091	2.74204

Substitution of bulkier R groups on the diketone was found to influence the reaction rate and the product distribution. As the data show, the reaction rate generally slows with increased branching in the aliphatic functional groups. This is consistent with increasing

[3] PCGAMESS version 7.0 was used to determine the optimized geometry in the gas-phase and the thermochemical data [20]. GAMESSPLUS version 4.7 was used to calculate the solvation energy [21]. Based on the general atomic and molecular electronic structure system (GAMESS) as described in [22].

[4] Computational parameters for the diketo and enol tautomers of **1a** and **1g** are available as the supplemental material at http://www.interscience.wiley.com/jpages/0538-8066/suppmat/.

steric crowding, both in the formation of the phenylhydrazones as well as in the transition state in the rate-determining step of the reaction. Steric effects play a role in formation of the aromatic-substituted pyrazoles since free rotation around the bond joining the aromatic ring and the carbonyl carbon undoubtedly causes steric crowding in the transition state, raising the activation energy. Likewise, increasing the bulk of the R group on the diketone leads to formation of pyrazole product **3** in larger proportion than **2**. Steric and stereoelectronic factors in the initial nucleophilic addition step of phenylhydrazine to the diketone equilibrium mixture influence this preference.

When determining the reaction order with respect to the diketone, we noted a reversal in the product distribution if excess diketone was present. A 2.4:1 preference for pyrazole **2**: pyrazole **3** was obtained. At present, it is unclear why this occurred.

Varying substituents on the aromatic trifluoromethyl-1,3-diketones was also studied. Here, we expected that electron-withdrawing groups (EWGs) on the phenyl ring of the diketone would enhance the reaction rate since the carbonyls would be more electron deficient. To evaluate substituent effects, the $\log(k_{P_T}/k_0)$ and $\log(k_{\mathbf{II}}/k_0)$ versus σ_{para} values were plotted (Fig. 2) for entries 7 and 11–15, yielding values of $\rho = +1.6$.

The data in Table I show that EWGs on the diketones accelerate the reaction by as much as a factor of 10. The small, positive value of ρ and the correlation of $\log(k/k_0)$ with σ_{para} and not σ^+ indicate that EWGs enhance the rate of product formation through induction for this series of reactions [23]. Finally, the fact that EWGs enhance the rate of phenylhydrazone intermediate loss at nominally the same rate as product formation is further evidence that ring closure is rate determining for pyrazole formation under these reaction conditions. If final dehydration of the pyrazoline intermediate **III** were rate determining, we would expect correlation with σ^+ since electron-donating groups (EDGs) could accelerate the dehydration mesomerically.

Effect of Phenylhydrazine Substituents on the Raction Rate and Product Distribution

The effect of hydrazine substituents on the reaction rate was also determined. If a phenylhydrazone intermediate **II** (Fig. 3) was involved in the rate-determining step, EDGs would enhance the nucleophilicity of the interior nitrogen and accelerate the reaction. The rates of product formation and phenylhydrazone (**II**) consumption (Fig. 4) were followed, and the data are presented in Table I.

As noted in the Experimental section, intermediates **II-2-2a, II-2-4a**, and **II-2-6a** were isolated and fully characterized. We observed arylhydrazones **II-3-3a, II-3-5a, II-3-7a, II-2-8a**, and **II-3-9a** in the ^{19}F NMR, but were unable to isolate them because of rapid cyclization and dehydration to the corresponding pyrazole upon removal of the solvent under reduced pressure. When the isolated intermediates were resubjected to reaction conditions, condensation rates were comparable to those shown in Table I (entries 1, 17, and 18) (see footnote 3).

Observed rate constants for pyrazole formation were determined, and the data are recorded in Table I. The $\log(k_{P_T}/k_0)$ and $\log(k_{\mathbf{II}}/k_0)$ versus σ_{para} were plotted (Fig. 5), giving slopes (ρ) of -2.3 for both arylhydrazone consumption and pyrazole formation.

As the data show, the reaction is more highly sensitive to substituents on the phenylhydrazine than the aryl diketone. The order of reactivity was, as expected, 4-methoxyphenylhydrazine > phenylhydrazine > 4-nitrophenylhydrazine > 2,4-dinitrophenylhydrazine, with rates varying nearly 400-fold. The magnitude and negative value of ρ coupled with the fact that $\log(k_{P_T}/k_0)$ and $\log(k_{\mathbf{II}}/k_0)$ do not correlate with σ^+ or σ^- for this process indicate that EDGs increase the rate of intermediate loss and product formation through induction by the same amount, in accord with rate-determining ring formation. This is corroborated by our finding that cyclization rates of the isolated arylhydrazones compared favorably with product formation kinetic data presented in Tables I and II.

While product distribution does not appear to be modulated greatly by substituents on the phenylhydrazine, excess phenylhydrazine leads to rapid formation of pyrazole **3** to the near exclusion of pyrazole **2**. The intermediate **II-2** was, however, present in solution and when induced to close under elevated temperature, led to a final product ratio of 2.3 (pyrazole **2**):1 (pyrazole **3**).

Effect of Acidity on Product Distribution and the Reaction Rate

The nature of acid catalysis in pyrazole formation has received little attention. While general acid catalysis is often observed for nucleophilic addition of amines to carbonyl species [23–26], the behavior is often complex. Uncatalyzed rate-limiting addition to the carbonyl species is found in cases of moderately basic nucleophiles. Acid concentrations that allow for optimal protonation of the electrophile will maximize the rate, but continued increases in the acidity to a point where all species are protonated will slow the reaction. Likewise, when the acid concentration is decreased to a

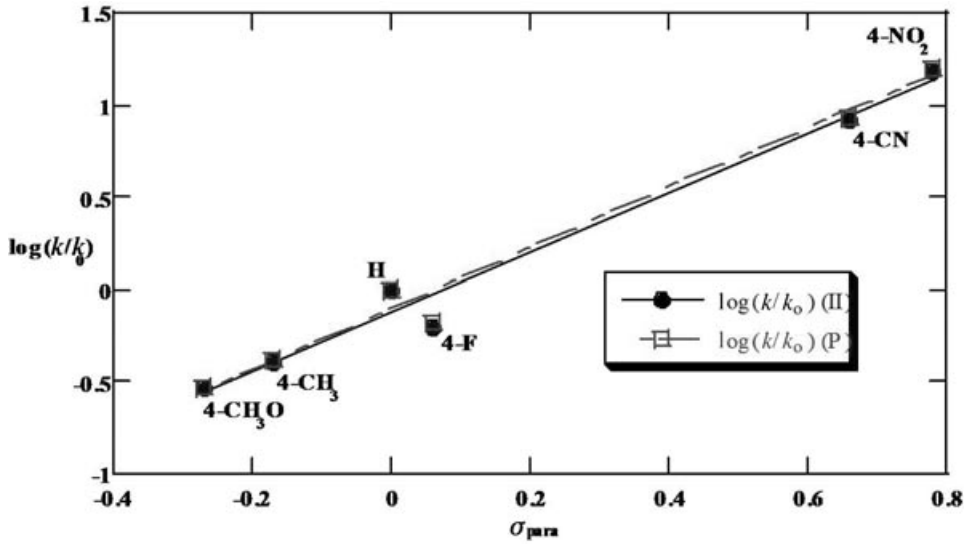

Figure 2 $\log(k_{P_T}/k_0)$ and $\log(k_{\mathbf{II}}/k_0)$ versus σ_{para} for substituted aryl trifluoromethyl-1,3-diketones.

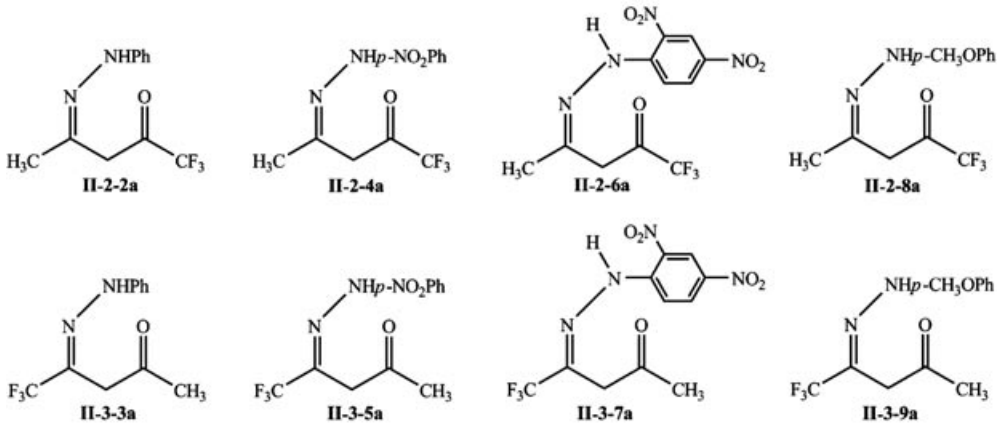

Figure 3 Arylhydrazone intermediates.

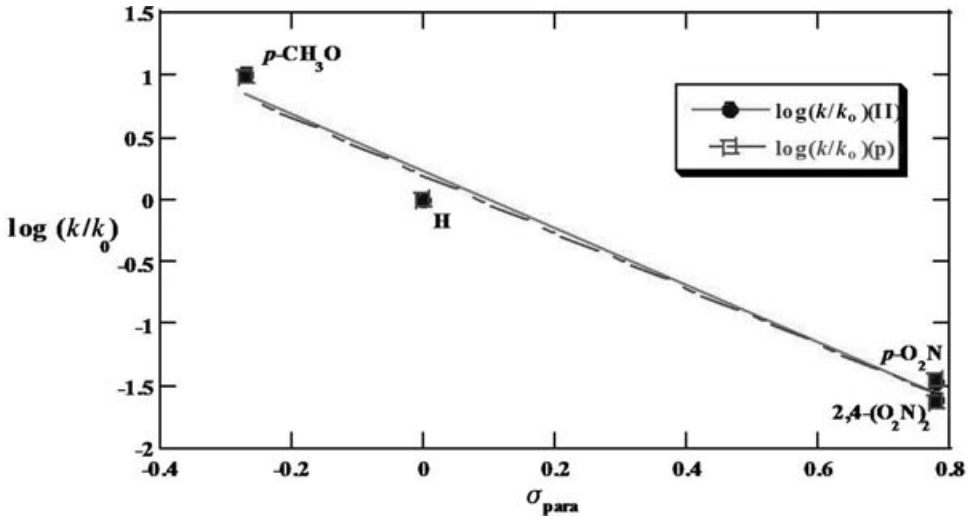

Figure 4 $\log(k_{P_T}/k_0)$ and $\log(k_{\mathbf{II}}/k_0)$ versus σ_{para} for condensation of **1a** with substituted phenylhydrazines.

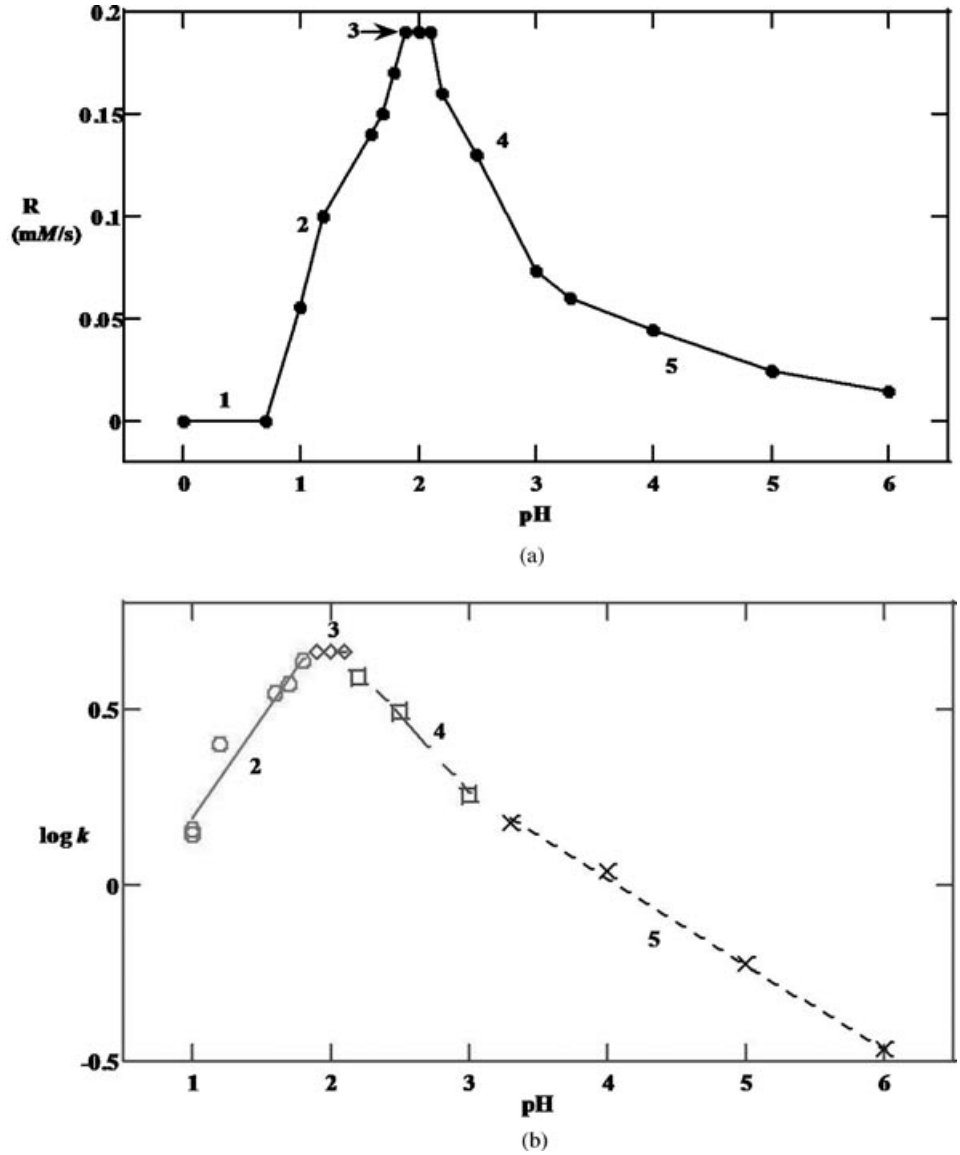

Figure 5 Pyrazole formation pH profile. (a) Product formation rate versus pH. (b) log k versus pH.

point insufficient to protonate the carbonyl undergoing nucleophilic attack and promote elimination of water, the reaction will again slow. We anticipated a response similar to this for pyrazole formation.

Using diketone **1a** and phenylhydrazine, an acidity profile for pyrazole formation was determined. The results are compiled in Table IV and are presented in graphical form in Fig. 5.

Acidity of the reaction medium appears to have two effects. First, minor changes in the acidity modulate product regioselectivity. At pH >1.6, a preference for pyrazole **3** is shown. Below this pH, pyrazole **2** gains predominance.

Second, small pH adjustments produce sizeable changes to the reaction rate. As Fig. 5a shows, pyrazole formation demonstrates a rate-acidity curve with five distinct regions and is similar to other carbonyl addition reactions with moderately basic amines [23,25,26]. In region 1 (pH 0 $\leq$.7), the reaction is completely inhibited by protonation of the phenylhydrazine. From pH $>$ 0.7 $<$ 1.9 (region 2), the reaction may be partially inhibited by either protonation of the phenylhydrazine or of the innermost phenylhydrazone nitrogen.

This reaction reaches a maximum rate in region 3 (pH 1.9–2.1), ruling out catalysis by the conjugate acid of phenylhydrazine since that would require a rate

Table IV Pyrazole Formation Rate Dependence on Acidity

pH	dP/dt (mM s)	k_{obs} (1 mM s^{-1})	log (k)	Product Ratio (**2:3**)
0.0	0.00	0.00	–	–
0.7	0.00	0.00	–	–
1.0[a]	0.056 (0.055)	1.4 (1.38)	0.146 (0.140)	7:5
1.2	0.10	2.5	0.398	
1.6	0.14	3.5	0.544	1:1
1.7	0.15	3.7	0.568	
1.8	0.17	4.3	0.633	
1.9	0.19	4.8	0.663	
2.0[a]	0.19 (0.19)	4.8 (4.8)	0.663 (0.663)	1:20
2.1	0.19	4.8	0.663	
2.2	0.16	3.9	0.591	
2.5	0.13	3.1	0.491	
3.0[a]	(0.073)	(1.8)	(0.255)	1:25
3.3[a]	(0.060)	(1.5)	(0.176)	
4.0[a]	(0.044)	(1.1)	(0.041)	0:100
5.0[a]	(0.024)	(0.60)	(−0.222)	
6.0[a]	(0.014)	(0.34)	(−0.469)	

Entries for buffer studies are in parentheses.

[a] pH maintained by HCl buffer (pH 1 and 2) and acetate buffer (pH 3, 4, 5, and 6), ionic strength 1.0 M.

maxima at $pH = pK_a \sim 5.2$ [25,26]. Buffer studies conducted at pH 2 show that the rate is not subject to general acid catalysis in this region. The reaction slows in region 4 ($pH > 2.1 \leq 3$), but a sufficient quantity of acid is available for product formation. At $pH \geq 3$ (region 5), insufficient protonation of the carbinolamine intermediate **I**, slower dehydration to intermediate **II**, and dehydration of intermediate **III** lead to slower pyrazole formation rates.

Figure 5b provides several pieces of information. First, the buffer studies[5] and linearity of the plot in region 5 are suggestive of general acid catalysis. We note in this pH range a Bronsted coefficient of −0.24, indicating a small degree of proton transfer in the rate-determining step. At low-acid concentrations, intramolecular proton transfers predominate, slowing the reaction rate, with rate-limiting dehydration to the pyrazole likely at $pH > 3$. In support of this, a hydroxypyrazoline intermediate (**III-2-4a**) was isolated [11] (Fig. 6) and characterized by NMR at pH 6. As Norris and coworkers [10] noted, dehydration to the pyrazole was slow under these conditions; heating or addition of acid was required for quantitative production. This finding is consistent with our acidity profile.

Region 4 yields a Brønsted coefficient of −0.43, possibly revealing a shift in the reaction pathway or change in the rate-determining step. In this pH range, we surmise that the increased acid concentration

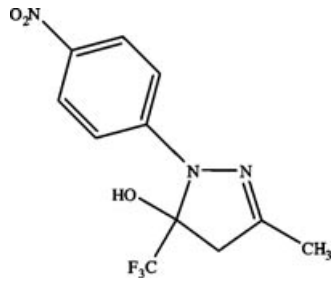

Figure 6 Pyrazoline intermediate **III-2-4a**.

speeds up the final dehydration step to a point equivalent to the rate of intermediate **II** consumption.

In region 3, we find a slope = 0, indicating a change in the rate-determining step from that previously discussed to an uncatalyzed rate-determining nucleophilic addition to the phenylhydrazone carbonyl. Under these conditions, sufficient acid is present for both inter- and intra-molecular proton transfers to promote formation of the transient pyrazoline intermediate **III** and rapid dehydration to the pyrazole products. Buffered solution studies at pH 2 showed no rate acceleration over the unbuffered solution, in accord with an uncatalyzed process.

In region 2, the Brønsted coefficient of 0.56 shows a higher degree of proton transfer in the rate-determining step. However, the reversal of slope again indicates a shift in the reaction pathway. The reaction slows, likely inhibited due to increased protonation of the nucleophilic species. Complete inhibition was found from pH 0.7 to 0.0 when [acid] ≥ [phenylhydrazine].

[5] pH was maintained by HCl buffer (pH 1 and 2) and acetate buffer (pH 3, 4, 5, and 6), ionic strength 1.0 M.

Proposed Mechanisms of Pyrazole Formation

Previously, we reported that unsymmetric trifluoromethyl-1,3-diketones exist primarily in a tautomeric equilibrium between the diketone (K) and two chelated cis-enolic forms (E_1 and E_2) in protic solvents like ethanol [27–29]. In acidic, ethanolic solutions and prior to addition of phenylhydrazine, ^{19}F NMR confirms the presence of these tautomers (Fig. 1a), a finding supported by K_{eq} values for the tautomers obtained from ab initio computations in Table III [20–22].

Determination of the species undergoing nucleophilic attack by phenylhydrazine is challenging, requiring consideration of several pieces of evidence. Figure 7 depicts the six possible routes of nucleophilic addition to these electrophilic species by arylhydrazines leading to pyrazoles **2** and **3**—two Michael-type additions (E_1-M_3 and E_2-M_1), and four carbonyl additions (K-C_1, K-C_3, E_1-C_1, and E_2-C_3).

While it is statistically more likely that nucleophilic addition to the carbonyl would occur, the borderline softness of the arylhydrazine bases [23] in this series of reactions suggests that Michael-type additions might also take place. Linderman and Kirollos [9] proposed an analogous mechanism for nucleophilic additions of hydrazines to propargyl trifluoromethyl ketones.

Identification of intermediates **II-2** and **II-3** implicates the diketo form as a likely electrophilic species in this process, but Michael-fashion addition to the enols by phenylhydrazine cannot be ruled out. Finally, ^{19}F spectral data show that upon addition of phenylhydrazine, both the diketone and enol resonances are depleted within 90 s, lending support to the idea that the enols and the diketo form may undergo nucleophilic addition. It is unknown whether the enol depletion occurs due to Michael-fashion addition, nucleophilic attack at the carbonyl, or an enol → keto equilibrium shift.

In light of these results, we are now prepared to provide some mechanistic detail of the condensation leading to pyrazole **3**. Scheme 3 summarizes reactions of the diketo form, enol 2, and Michael-fashion attack of enol 1 tautomers with phenylhydrazine in acidic media where A-H is any general acid and B refers to any general basic species in the solution. An analogous mechanism involving the other carbonyl of the diketo form, enol 1, and Michael-fashion attack of enol 2 leads to pyrazole **2**.

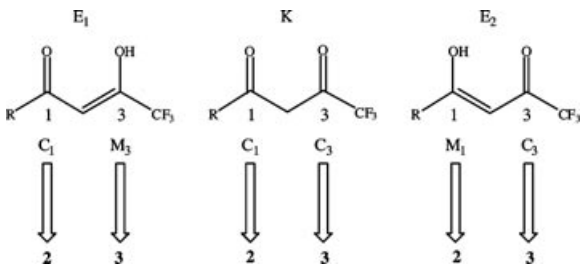

Figure 7 Nucleophilic addition routes.

Stage 1 is a preequilibrium between the arylhydrazine and acid, leading to complete inhibition of the condensation when [acid] ≥ [arylhydrazine]. At lower acid concentrations, the second stage of the reaction commences via a preassociative complex consisting of the phenylhydrazine, diketone, and acid, similar to the complex proposed for acid-catalyzed hydrazine additions to ketones [19,23,25,26]. We include not only nucleophilic addition to the carbonyl of the diketone and enol 2 tautomers but also a Michael-fashion attack on enol 1 as well, since that possibility cannot be ruled out. A common intermediate in this stage of the pathway is the initial amino-alcohol adduct, **I**. Intermediate **I** was identified in the reaction medium, but undergoes dehydration to intermediate **II** too rapidly to isolate. The numerous proton transfers that occur during this reaction are likely both inter- and intramolecular below pH 2, with intramolecular proton transfers becoming dominant as the acid concentration drops [23,25,26]. At pH 2.0, the initial nucleophilic addition is rapid and assisted by protonation. Dehydration of **I** gives rise to intermediate **II**, which was identified.

The third stage contains the rate-determining ring formation step at pH 2.0, apparently not acid catalyzed, and a series of rapid proton transfers leading to the pyrazoline intermediate **III**, also identified and in one case, isolated. Pyrazoline formation occurs as a result of intramolecular addition of the phenylhydrazone to the carbonyl. This pyrazoline formation is consistent with the observation that EWGs on aromatic rings of the diketones and EDGs on phenylhydrazine enhance the rate of intermediate **II** disappearance. Finally, the pH profile confirms that the rate of this second nucleophilic addition slows under conditions of low pH where protonation of **II** becomes significant, possibly giving rise to the inhibition route.

The final stage of the mechanism contains the dehydration of intermediate **III** to the heterocyclic products. At high concentrations of acid, this step is extremely fast, as evidenced by the transient nature of the pyrazoline intermediate, whose disappearance was monitored by ^{19}F NMR [10]. As the solution is made less acidic, however, this dehydration becomes rate limiting. The isolation and characterization of several pyrazoline intermediates in neutral media support this finding [10].

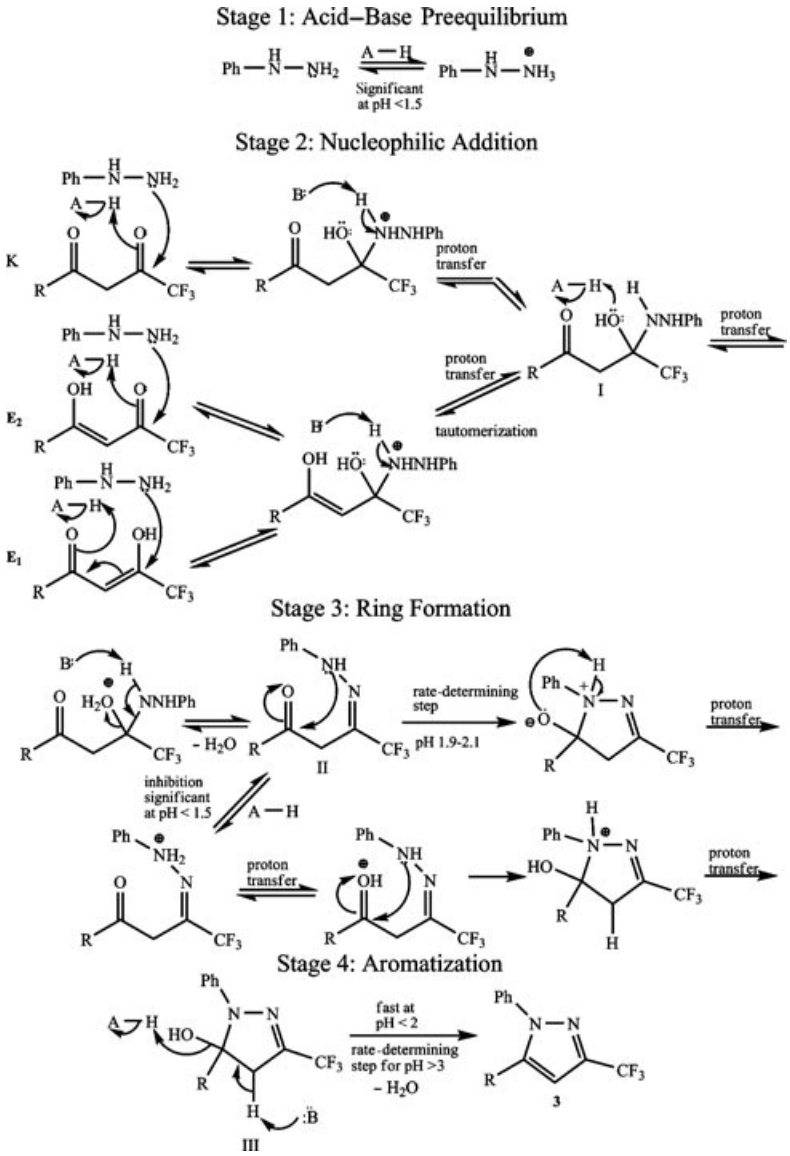

Scheme 3 Proposed pyrazole formation mechanism.

CONCLUSION

This kinetics study of pyrazole formation has yielded quantitative information regarding how substituents and acidity influence product regioselectivity, reaction rate, and the pathway for this important condensation involving arylhydrazines and 1,3-diketones. Comparing our results obtained in acidic media at room temperature to that found in the literature reveals several differences as well as a number of similarities.

Previous qualitative kinetics studies of pyrazole formation from arylhydrazines and β-dicarbonyl species or their derivatives have generally fallen into two categories: those conducted under basic, neutral, or acidic conditions in polar media while refluxing [10–12,14] and those examined at elevated temperature under neutral conditions followed by acid catalysis in nonpolar solvents [13].

We find that pyrazole regioselectivity is influenced by a combination of steric effects, reactant ratios, and acidity. Bulky substituents on the diketone increase the proportion of pyrazole **3**, whereas excesses of either the diketone or phenylhydrazine increase the proportion of pyrazole **2**. Similarly, Fernández and colleagues [13] reported that phenylhydrazine added to the less highly substituted electrophilic site in

condensations with highly strained norbornene-fused ring hydroxymethyleneketones in toluene and catalytic acid conditions leading to a pyrazole **3-**like compound.

Product regioselectivity was also found to be modulated by adjustments in the acidity of the reaction medium. Maintaining a pH > 1.7 optimizes the proportion of pyrazole **3**, while more acidic conditions lead to larger quantities of pyrazole **2**. In accord with our findings, Singh and coworkers [11,14] also showed that pyrazole **2** was the major isomer produced under highly acidic conditions and regioisomeric pyrazoles (pyrazole **3** predominating) are produced when phenylhydrazine was used in neutral or basic condensation conditions in ethanol.

We find that the rate of pyrazole formation is sensitive to substituents and acidity as well. Alkyl-substituted diketones react more rapidly than aryl diketones. Aryl diketones containing EWGs react more rapidly than unsubstituted or EDG-substituted cases. Phenylhydrazines containing EDGs accelerate pyrazole formation by enhancing the nucleophilicity of the phenylhydrazine's interior nitrogen during the cyclization step. The acidity profile indicates that an optimal reaction rate is observed at ca. pH 2.0 for the condensation at 0.20-M reactant concentrations in 95% ethanol at room temperature. In contrast, researchers examining pyrazole formation under basic or nonpolar solvent conditions found that heat or acid catalysis was necessary to force the condensation to completion [11,13].

Within the pH range studied, the reaction follows second-order kinetics, first order in phenylhydrazine, and first order in the diketone. The pH profile shows a complex dependence on acidity marked by inhibition of the reaction at low pH, a narrow uncatalyzed region, and at higher pH values, a region of general acid catalysis [23,25,26]. Knowledge of the diketone tautomeric equilibrium in the reaction medium, identification of key intermediates along the reaction pathway which are consistent with the experimental rate data coupled with the Hammett correlations support a mechanism that involves a rate-determining ring-closure step in the condensation of trifluoromethyl-1,3-diketones with arylhydrazines under acidic conditions.

The possibility that both the keto and enol forms react cannot be ruled out since the enol and keto tautomeric forms are present and rapidly disappear under reaction conditions [14], to give mixtures of pyrazoles.

Modulation of acidity shifts the rate-determining step. In region 2 (Fig. 5b), rate-determining ring formation is observed with some inhibition by acid; in region 3 this inhibition is minimal and leads to uncatalyzed ring closure. In region 4, the loss rates of intermediates **II** and **III** are competitive. The clear drop in the magnitude of log k in region 5 indicates a change to rate-limiting dehydration of **III**. This finding is consistent with the work of Penning et al. [3] and Singh et al. [11], who concluded that dehydration of intermediate **III** was rate determining in basic and neutral media.

Under basic conditions, different pathways could be available. von Auwers and Schmidt [18] reported hydrazone intermediates from the condensation of β-ketoaldehydes with phenylhydrazine, whereas Katrizky and coworkers [12] observed (by ^{1}H NMR) and isolated hydrazone intermediates arising from the condensation of β-ketoesters with phenylhydrazine enroute to pyrazolinones ca. pH 9. On the other hand, dihydroxypyrazolidine intermediates, such as those shown in Fig. 8, have also been identified by low-temperature NMR by Zefirov [15] (**a**), and in one instance, isolated under mildly basic conditions (b) [30]. It is plausible that intermediates like those in Fig. 8 may form during base-promoted condensations of highly electrophilic diketones with the more nucleophilic hydrazine. Under these conditions, the second nucleophilic addition step may be competitive with the initial dehydration step of **I** → **II** in our proposed mechanism, since dehydration might be retarded for a period of time sufficient to form dihydroxypyrazolidine intermediates. Nevertheless, neither we nor Norris and coworkers [10] found evidence supporting intermediates of the type in Fig. 8 for this condensation in acidic media.

The addition of our pyrazole formation kinetics study to the previous investigations conducted in neutral and basic media gives a more complete description of this condensation over a wide pH range. Scheme 3 provides a picture of pyrazole formation from diketone and phenylhydrazine under acidic conditions that is consistent with the kinetics, the presence of identified intermediates, Hammett plots, and pH profile.

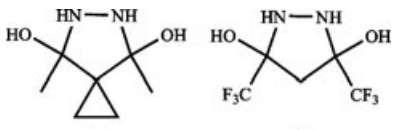

Figure 8 Dihydroxypyrazolidine intermediates.

The authors would like to thank the USMA Center for Molecular Science for computational support and the North Carolina State University and Edgewood Chemical and Biological Command NMR facilities for NMR support.

BIBLIOGRAPHY

1. Genin, M.; Biles, C.; Keiser, B. J.; Poppe, S. M.; Swaney, S. M.; Tarpley, G.; Yagi, T.; Romero, D. L. J Med Chem 2000, 43, 1034.
2. Guzman-Perez, A.; Wester, R. T.; Allen, M. C.; Brown, J. A.; Buchholz, A. R.; Cook, E. R.; Day, W. W.; Hamanaka, E. S.; Kennedy, S. P.; Knight, D. R.; Kowalczyk, P. J.; Marala, R. B.; Mularski, C. J.; Novomisle, W. A.; Ruggeri, R. B.; Tracey, W. R.; Hill, R. J. Bioorg Med Chem Lett 2001, 11(6), 803.
3. Penning, T. D.; Talley, J. J.; Bertenshaw, S. R.; Carter, J. S.; Collins, P. W.; Docter, S.; Graneto, M. J.; Lee, L. F.; Malecha, J. W.; Miyashiro, J. M.; Rogers, R. S.; Rogier, D. J.; Yu, S. S.; Anderson, G. D.; Burton, E. G.; Cogburn, J. N.; Gregory, S. A.; Koboldt, C. M.; Perkins, W. E.; Seibert, K.; Veenhuizen, A. W.; Zhang, Y. Y.; Isakson, P. C. J Med Chem 1997, 40, 1347.
4. Ware, G. W.; Whitcare, D. M. Introduction to insecticides. In: The Pesticide Book, 6th ed.; MeisterPro Information Resources: Willoughby, OH, 2004; p. 10.
5. Stiefel, J. Unpublished research, United States Military Academy, 1993.
6. Sloop, J. C.; Bumgardner, C. L. J Fluorine Chem 1992, 56, 141.
7. Sloop, J. C.; Bumgardner, C. L.; Loehle, W. D. J Fluorine Chem 2002, 118, 135.
8. Ishikawa, N. Bull Chem Soc Jpn 1981, 59, 3221.
9. Linderman, R. J.; Kirollos, K. Tetrahedron Lett 1989, 30(16), 2049.
10. Norris, T.; Colon-Cruz, R.; Ripin, D. H. Org Biomol Chem 2005, 3, 1844.
11. Singh, S. P.; Kumar, D.; Batra, H.; Naithani, R.; Rozas, I.; Elguero, J. Can J Chem 2000, 78, 1109.
12. Katrizky, A. R.; Barczynski, P.; Ostercamp, D. L. J Chem Soc, Perkin Trans II 1987, 969.
13. Fernández, F.; Caamaño, O.; García, M. D.; Alkorta, I.; Elguero, J. Tetrahedron 2006, 62, 3362.
14. Singh, S. P.; Kumar, V.; Aggarwal, R.; Elguero, J. J Heterocyclic Chem 2006, 43, 1003.
15. Zefirov, N. S.; Kozhushkov, S. I.; Kuznetsova, T. S.; Ershov, B. A.; Selivanov, S. I. Tetrahedron 1986, 42, 709–713.
16. Alberola, A.; Calvo, L.; Gonzalez Ortega, A.; Sadaba, M. L.; Sanudo, M. C.; Garcia Granda, S.; Garcia Rodriguez, E. Heterocycles 1999, 51, 2675–2686.
17. Reid, J. C.; Calvin, M. J Am Chem Soc 1950, 72, 2948.
18. von Auwers, K.; Schmidt, W. Chem Ber 1925, 58, 528.
19. Moscovici, R.; Ferraz, J. P.; Neves, E. A.; Tognoli, M. I.; do Amaral, L. J Org Chem 1976, 41, 4093.
20. Nemukhin, A. V.; Grigorenko, B. L.; Granovsky, A. A. Moscow Univ Chem Bull 2004, 45(2), 75.
21. Chamberlin, A. C.; Pu, J.; Kelly, C. P.; Thompson, J. D.; Xidos, J. D.; Li, J.; Zhu, T.; Hawkins, G. D.; Chuang, Y.-Y.; Fast, P. L.; Lynch, B. J.; Liotard, D. A.; Rinaldi, D.; Gao, J.; Cramer, C. J.; Truhlar, D. G. University of Minnesota, 2005.
22. Schmidt, M. W.; Baldridge, K. K.; Boatz, J. A.; Elbert, S. T.; Gordon, M. S.; Jensen, J. H.; Koseki, S.; Matsunaga, N.; Nguyen, K. A.; Su, S. J.; Windus, T. L.; Dupuis, M.; Montgomery, J. A. J Comput Chem 1993, 14, 1347.
23. Lowry, T. H.; Richardson, K. S. Mechanism and Theory in Organic Chemistry, 3rd ed.; Harper & Row: New York, 1987; Vol. 150, pp. 702–709.
24. McMurry, J. Organic Chemistry, 6th ed; Brooks-Cole: Pacific Grove, CA; 2004; p. 698.
25. Jencks, W. P. J Am Chem Soc 1959, 81, 475.
26. Sayer, J. M.; Edman, C. J Am Chem Soc 1979, 101, 3010.
27. Reichardt, C. Solvents and Solvent Effects in Organic Chemistry, 3rd ed; Wiley-VCH: Weinheim, Germany, 2003; Vol. 107, pp. 329, 375.
28. Sloop, J. C.; Bumgardner, C. L.; Washington, G.; Loehle, W. D.; Sankar, S. S.; Lewis, A. B. J Fluorine Chem 2006, 127, 780.
29. Ebraheem, K. A. K. Monatsh Chem 1991, 122, 157.
30. Elguero, J.; Yranzo, G. I. J Chem Res, Synop 1990, 120.